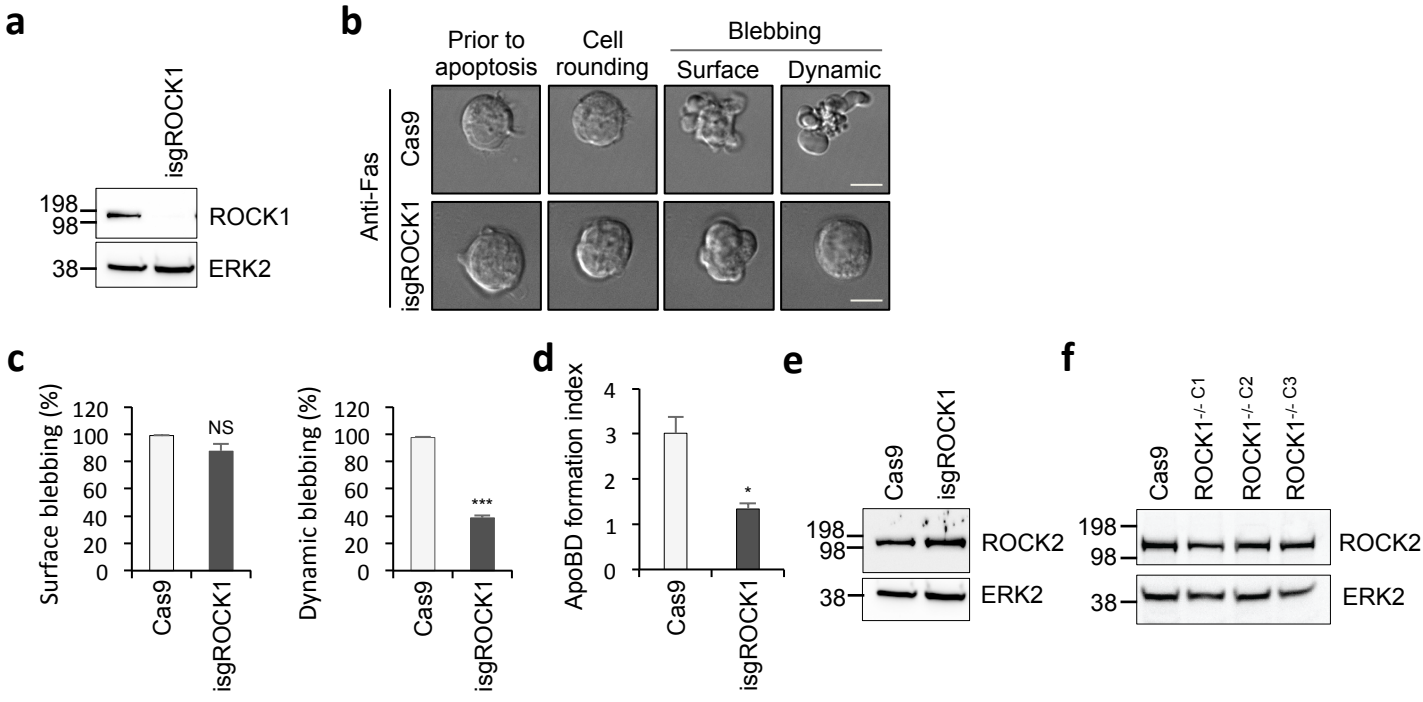
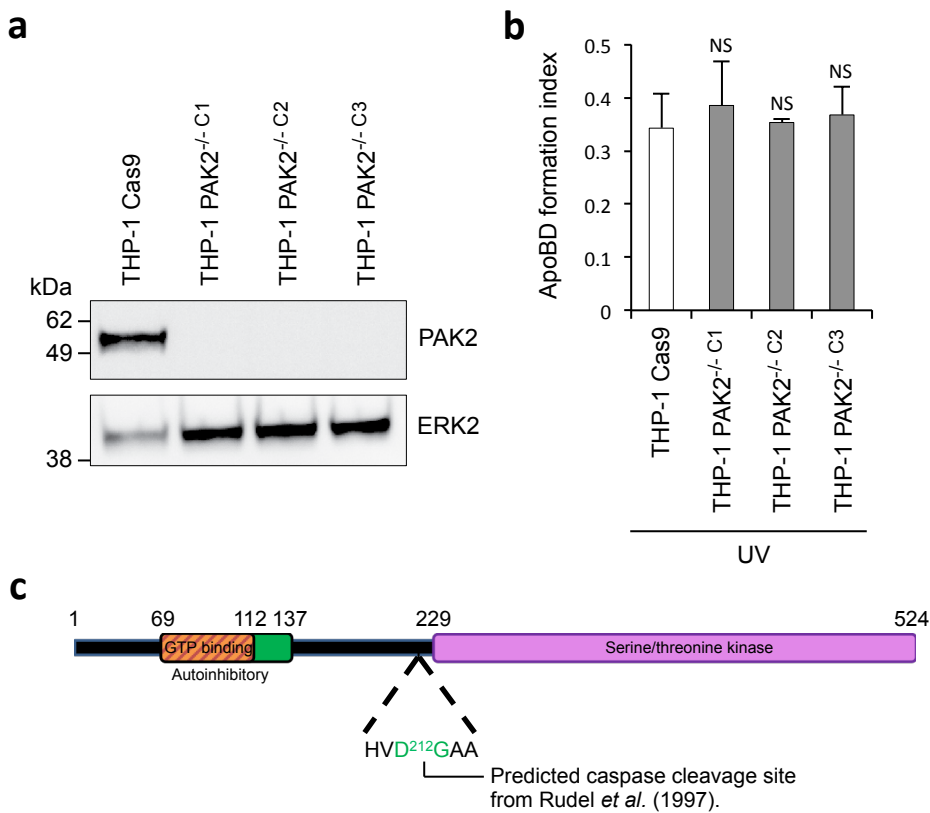


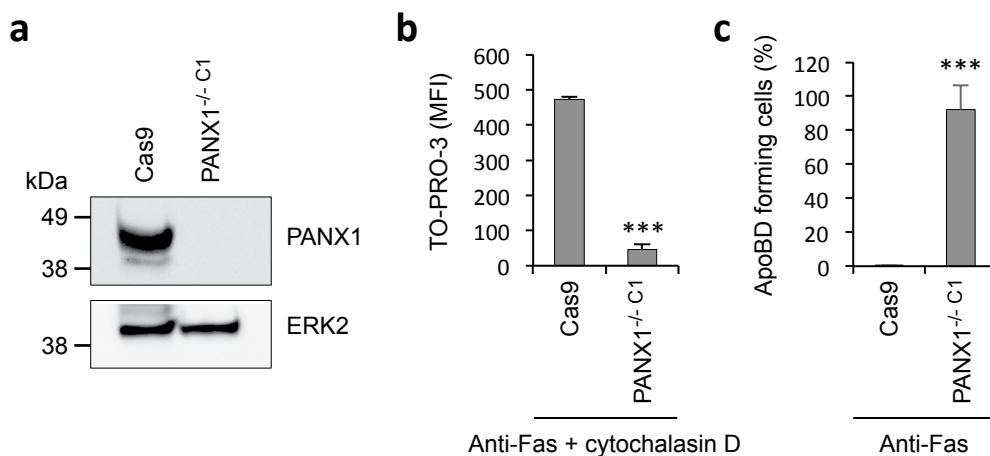
**Supplementary Figure 1. Treatment with PAK2 inhibitor FRAX1036 and LIMK1 inhibitor BMS-5 arrests cell cycle progression. (a)** Jurkat T cells treated with FRAX-1036 (2.5  $\mu$ M) for 24 h showed an increase in cells arrested in S-phase as determined by propidium iodide staining monitored by flow cytometry. **(b)** Jurkat T cells treated with BMS-5 (10  $\mu$ M) for 24 h showed an increase in cells arrested in G2-M phase as determined by propidium iodide staining monitored by flow cytometry. **(c)** Level of phosphorylated PAK2 (p-PAK2) was determined by immunoblot analysis of Jurkat T cells treated with vehicle (EtOH) or FRAX-1036 (2.5  $\mu$ M) for 0 to 4 h. **(d)** Level of phosphorylated cofilin (p-cofilin) was determined by immunoblot analysis of UV-irradiated (150 mJ/cm<sup>2</sup>) Jurkat T cells treated with vehicle (DMSO) or BMS-5 (10  $\mu$ M) for 0 to 4 h. Error bars represent s.e.m. Data represents three independent experiments. \*  $P < 0.05$ , \*\*  $P < 0.01$ , \*\*\*  $P < 0.001$ , NS =  $P > 0.05$ , unpaired Student's two-tailed  $t$ -test.



**Supplementary Figure 2. Loss of ROCK1 expression in Jurkat T cells impairs apoptotic membrane blebbing and ApoBD formation.** (a) Loss of ROCK1 protein expression with CRISPR/Cas9-mediated ROCK1 gene disruption in doxycycline (dox, 1  $\mu\text{g/ml}$ ) treated isgROCK1 Jurkat T cells was validated by immunoblot analysis. (b) Representative time-lapse DIC imaging of dox-treated Cas9 and isgROCK1 Jurkat T cells over 4 h post anti-Fas (0.5  $\mu\text{g/ml}$ ) treatment showing apoptotic morphology. (c) Quantification of apoptotic isgROCK1 cells that underwent surface and dynamic blebbing ( $n=3$ ). (d) Formation of ApoBDs from apoptotic isgROCK1 cells treated with anti-Fas (0.5  $\mu\text{g/ml}$ ) and trovafloxacin (40  $\mu\text{M}$ ), as measured by flow cytometry ( $n=3$ ). (e) Expression of ROCK2 in dox-treated Cas9 and isgROCK1 Jurkat cells and (f) ROCK1 knockout clonal cells, was monitored by immunoblot analysis. Error bars represent s.e.m. Scale bar, 10  $\mu\text{m}$ . Data represents three independent experiments. \*  $P<0.05$ , \*\*\*  $P<0.001$ , NS =  $P>0.05$ , unpaired Student's two-tailed  $t$ -test.

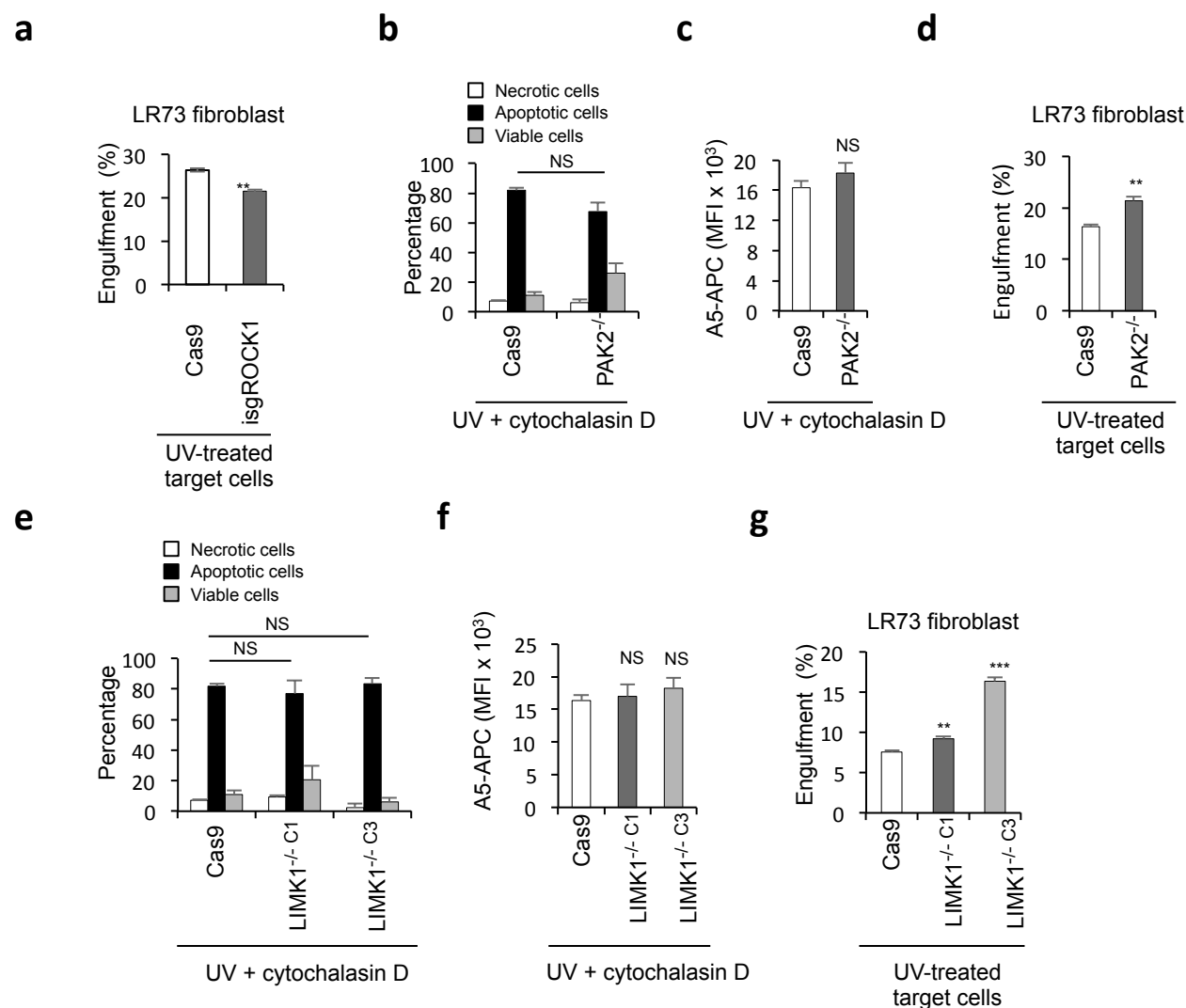


**Supplementary Figure 3. Loss of PAK2 in THP-1 monocytes does not impair ApoBD formation.** (a) Loss of PAK2 protein expression with CRISPR/Cas9-mediated PAK2 gene disruption in three THP-1 cell clonal populations (THP-1 PAK2<sup>-/-</sup> C1, THP-1 PAK2<sup>-/-</sup> C2, THP-1 PAK2<sup>-/-</sup> C3) was validated by immunoblot analysis. (b) Formation of ApoBDs from UV irradiated THP-1 PAK2<sup>-/-</sup> cells, as monitored by flow cytometry (n=3). (c) Schematic representation of human PAK2. Key functional domains and the predicted caspase cleavage site from Rudel *et al.* (1997) shown. THP-1 Cas9, THP-1 cells expressing Cas9 only was used as a control. (b) Error bars represent s.e.m. Data are representative of three independent experiments. NS =  $P > 0.05$ , unpaired Student's two-tailed *t*-test.

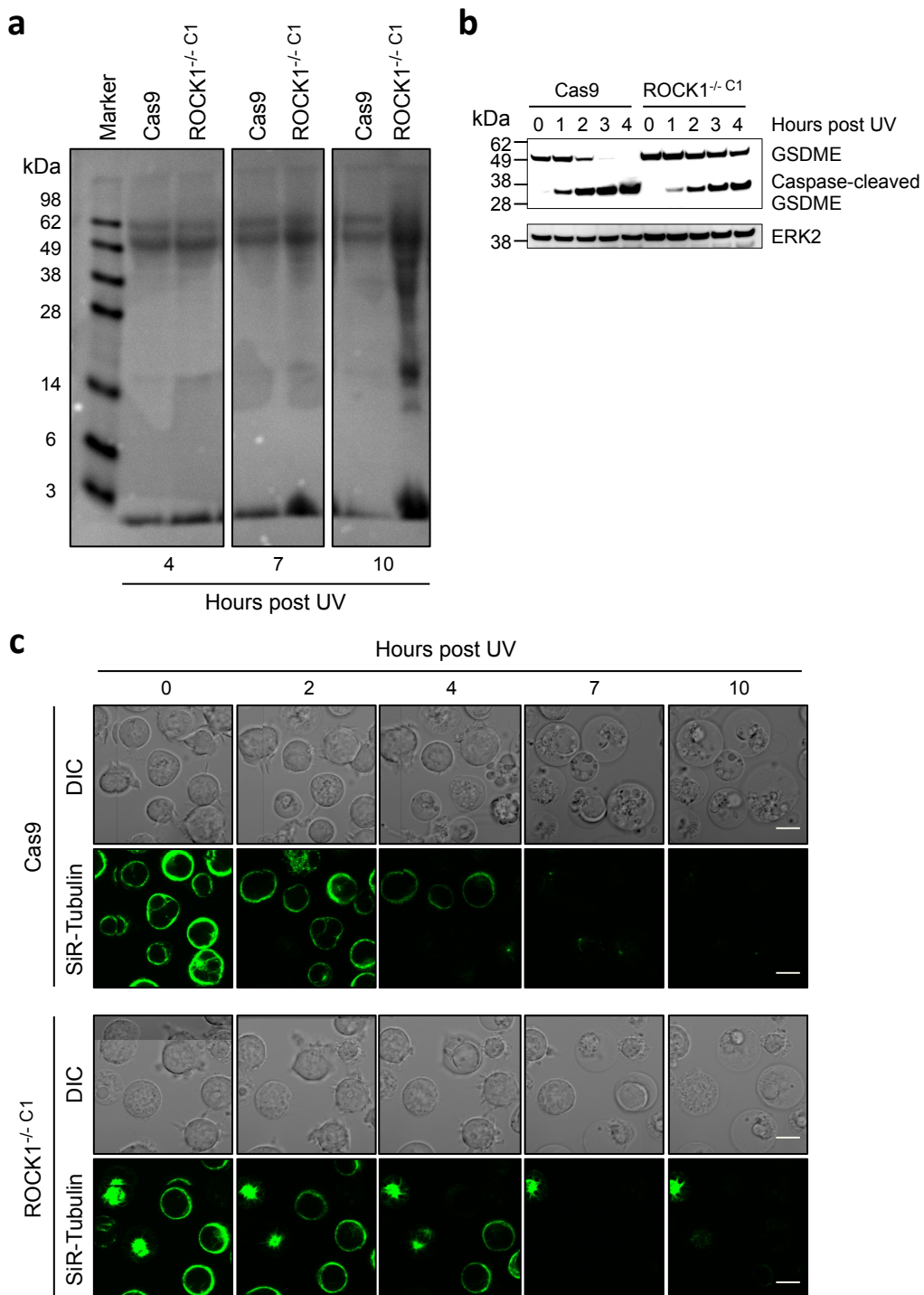


**Supplementary Figure 4. Loss of PANX1 expression enhances ApoBD formation.** (a) Loss of PANX1 protein expression with CRISPR/Cas9-mediated PANX1 gene disruption in Jurkat T cell clonal population (PANX1<sup>-/-</sup> C1) was validated by immunoblot analysis. (b) Reduction in TO-PRO-3 uptake (a nucleic acid dye that enters apoptotic Jurkat T cells via caspase-activated PANX1 channels) in apoptotic PANX1<sup>-/-</sup> C1 cells, as measured by flow cytometry. Cells were treated with anti-Fas (0.5 µg/ml) to induce apoptosis and cytochalasin D (10 µM) to prevent the disassembly of apoptotic cells in all samples to ensure fair comparison between cell lines (n=3). (c) Formation of ApoBDs from PANX1<sup>-/-</sup> C1 cells treated with anti-Fas (0.5 µg/ml) to induce apoptosis, as measured by flow cytometry (n=3). Cas9, Jurkat T cells expressing Cas9 only was used as a control. (b and c) Error bars represent s.e.m. Data are representative of at least three independent experiments. \*\*\*  $P < 0.001$ , unpaired Student's two-tailed  $t$ -test.

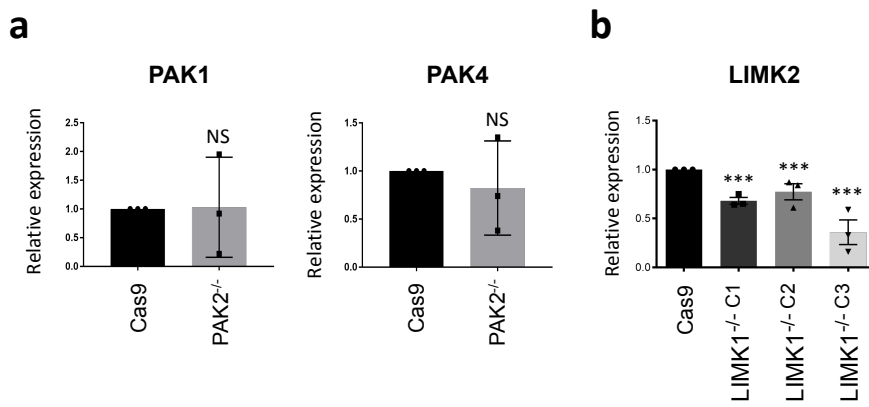




**Supplementary Figure 6. Loss of PAK2 and LIMK1 does not lead to a defect in efferocytosis by fibroblast cells** (a) Quantitation of the uptake of UV-treated CypHer5E-stained non-clonal Cas9, isgROCK1 cells by CellTrace Violet-stained hamster LR73 fibroblast cells as determined by flow cytometry. (b) Level of necrotic, apoptotic and viable cells were determined in UV-treated PAK2<sup>-/-</sup> cells in the presence of cytochalasin D (10  $\mu$ M) by flow cytometry (n=3), and (c) PtdSer exposure on apoptotic PAK2<sup>-/-</sup> based on A5-PE staining as determined by flow cytometry (n=3), (d) Quantitation of the uptake of UV-treated CypHer5E-stained Cas9, PAK2<sup>-/-</sup> cells by CellTrace Violet-stained hamster LR73 fibroblast cells as determined by flow cytometry. (e) Level of necrotic, apoptotic and viable cells were determined in UV irradiated LIMK1<sup>-/-</sup> C1 and LIMK1<sup>-/-</sup> C3 cells in the presence of cytochalasin D (10  $\mu$ M) by flow cytometry (n=3), and (f) PtdSer exposure on apoptotic LIMK1<sup>-/-</sup> C1 and LIMK1<sup>-/-</sup> C3 based on A5-PE staining as determined by flow cytometry (n=3), (g) Quantitation of the uptake of UV-irradiated CypHer5E-stained Cas9, LIMK1<sup>-/-</sup> C1 and LIMK1<sup>-/-</sup> C3 cells by CellTrace Violet-stained hamster LR73 fibroblast cells as determined by flow cytometry. Data are representative of at least three independent experiments. \*\*  $P < 0.01$ , \*\*\*  $P < 0.001$ , NS =  $P > 0.05$ , unpaired Student's two-tailed  $t$ -test.



**Supplementary Figure 6. Early onset of secondary necrosis in ROCK1<sup>-/-</sup> Jurkat T cells is independent of GSDME and microtubule network function in apoptosis.** (a) Ponceau stain of western-transferred precipitated supernatant proteins of Cas9 and ROCK1<sup>-/-</sup> C1 Jurkat T cells at 4, 7 and 10 h post UV (150 mJ/cm<sup>2</sup>) induced apoptosis. (b) Immunoblot analysis of GSDME expression and cleavage in UV-treated (150 mJ/cm<sup>2</sup>) Cas9 and ROCK1<sup>-/-</sup> C1 Jurkat T cells. (c) Representative time-lapse confocal microscopy images of UV-treated (150 mJ/cm<sup>2</sup>) Cas9 and ROCK1<sup>-/-</sup> C1 Jurkat T cells stained with SiR-Tubulin to monitor microtubules during the progression of apoptosis. Scale bar, 10  $\mu$ m. Data are representative of three independent experiments.



**Supplementary Figure 7. PAK2 and LIMK1 knockout Jurkat T cells express corresponding isoforms. (a)** Quantitative PCR (qPCR) analysis of PAK2<sup>-/-</sup> cells showed no significant change in PAK1 and PAK4 expression as compared to Cas9 control ( $n=3$ ). **(b)** LIMK1<sup>-/-</sup> cells showed a reduction in the expression of LIMK2 mRNA as determined by qPCR analysis ( $n=3$ ).  $\Delta\Delta\text{CT}$  method was used to analyze qPCR data. Error bars represent s.e.m. Data represents three independent experiments. \*\*\*  $P<0.001$ , NS =  $P>0.05$ , unpaired Student's two-tailed  $t$ -test.